Enlarged right-sided dimensions and fibrosis of the right ventricular insertion point on cardiovascular magnetic resonance imaging is seen early in patients with pulmonary arterial hypertension associated with connective tissue disease

Hesselstrand, Roger; Scheja, Agneta; Wuttge, Dirk; Arheden, Håkan; Ugander, Martin

Published in:
Scandinavian Journal of Rheumatology

DOI:
10.3109/03009742.2010.507217

2011

Enlarged right sided dimensions and fibrosis of the right ventricular insertion point on cardiovascular magnetic resonance imaging is seen early in patients with pulmonary arterial hypertension associated with connective tissue disease

Roger Hesselstrand MD, PhD[1]; Agneta Scheja MD, PhD[1]; Dirk M Wuttge MD, PhD[1]; Håkan Arheden MD, PhD[2]; Martin Ugander MD, PhD[2]

[1] Department of Rheumatology, Skåne University Hospital, Lund University, Lund, Sweden

[2] Department of Clinical Physiology, Skåne University Hospital, Lund University, Lund, Sweden

Running head: Findings on cardiovascular MRI in PAH and SSc

Correspondence to:

Roger Hesselstrand MD, PhD

Department of Rheumatology

Skåne University Hospital

Lund University

S-221 85 Lund, Sweden

Telephone: + 46 46 171620

Fax: + 46 46 128468

E-mail: roger.hesselstrand@med.lu.se

ABSTRACT

Objectives: To describe the findings of cardiovascular magnetic resonance imaging (CMR) in patients with pulmonary arterial hypertension (PAH) associated with connective tissue disease (CTD-PAH) and in consecutive patients with systemic sclerosis (SSc) without PAH.

Methods: The study comprised 9 consecutive patients who were admitted for right heart catheterization under the suspicion of CTD-PAH and 25 consecutive patients who were admitted for evaluation because of a clinical suspicion of SSc. In addition to the regular assessment, they also underwent examination by CMR.

Results: CMR measurements of right ventricular volumes and function showed severe pathology in patients with CTD-PAH. Patients with SSc without PAH had similar but much less severe findings. Right ventricular end diastolic volume and right ventricular ejection fraction were abnormal in all patients with CTD-PAH. In 8 out of 9 patients with CTD-PAH, fibrosis was seen in the right ventricular insertion point, likely caused by increased tension, but only in one of the consecutive SSc patients. This patient was diagnosed with CTD-PAH 20 months later.

Conclusions: In CTD-PAH, CMR shows severe changes in right ventricular volumes and function, but also fibrosis in the right ventricle insertion point. Similar abnormalities, although much less severe, may be seen already at diagnosis of SSc. Further evaluation is warranted to determine whether these findings are of value to screen for early signs of PAH in SSc.

Key words: systemic sclerosis, scleroderma, magnetic resonance imaging, fibrosis, pulmonary hypertension

INTRODUCTION

Systemic sclerosis (SSc, scleroderma) is a systemic connective tissue disease characterised by fibrosis in skin and internal organs, progressive vascular obliteration and the production of auto antibodies [1]. SSc is associated with an increased mortality [2; 3; 4], but prognosis is extremely variable.

Pulmonary involvement, either fibrotic or vascular, has been the leading cause of death since the 1990's [3; 5; 6], and physicians taking care of SSc patients have enthusiastically modified their algorithm for investigation to address this issue. However, assessing the cardiac involvement comprises several investigational techniques and is therefore more diverse. Nevertheless, both primary fibrotic and vascular involvement of the heart, as well as secondary involvement due to pulmonary arterial hypertension (PAH), have been extensively described.

The recommended investigation of cardiac involvement in SSc consists primarily of assessment of symptoms, a physical examination, chest x-ray, electrocardiogram and Doppler echocardiography [7].

Cardiovascular magnetic resonance imaging (CMR) has been used to describe cardiac abnormalities in cross sectional cohorts of SSc patients [8-13], pharmacological effects on myocardial perfusion in SSc patients [14] and in patients diagnosed with PAH or suspected PAH secondary to SSc [12, 15].

The aim of this study was to describe the findings of CMR in 2 groups of patients; consecutive patients with SSc (SSc no PAH) and patients with newly diagnosed PAH associated with connective tissue disease (CTD-PAH; group 1.3.1. in the Venice classification [16]).

SUBJECTS AND METHODS

Subjects

This study was performed during the time period from June 2006 to March 2008. In total 34 patients underwent examination with CMR. 25 consecutive patients were referred to our department for investigation because of a clinical suspicion of SSc and 9 had CTD-PAH. The diagnosis of SSc was made based on the ACR criteria [17] and subdivided into diffuse cutaneous SSc (dcSSc) or limited cutaneous SSc (lcSSc) according to the extent of skin involvement [1]. Out of the 25 patients, 2 were classified as dcSSc, 17 as lcSSc and 6 did not fulfil the ACR criteria because of mild or possibly early disease and were classified as suspected SSc (susp SSc). All 6 susp SSc patients reported Raynaud's phenomenon and swelling of hands, 4 of them had sclerodactyly and 4 were also positive for centromeric antibodies. Three of the susp SSc patients fulfilled the criteria for early SSc [18] and one year later 2 of them were classified as lcSSc. Disease duration was defined as time from the first non Raynaud's manifestation. In this study the first non Raynaud's manifestation was skin thickening of the fingers in all cases.

The 9 CTD-PAH patients consisted of patients who underwent right heart catheterization (RHC) on the suspicion of PAH, because of dyspnoea and echocardiographic signs of pulmonary hypertension. Of these, 6 had lcSSc, one polymyositis, one rheumatoid arthritis and one juvenile idiopathic arthritis.

Study design

The study was approved by the regional ethics committee and all patients provided written informed consent. All patients were examined according to our local guidelines, which include echocardiography, spirometry, chest x-ray and high resolution computed tomography of the lungs. CMR, and in cases of suspected PAH, RHC were done during the same week as the other examinations.

Right heart catheterisation

RHC was performed by experienced clinicians according to standard techniques, using a Swan-Ganz catheter. Mean right atrial pressure, systolic, diastolic, and mean pulmonary arterial pressure (mPAP), as well as pulmonary capillary wedge pressure (PCWP) were measured. Cardiac output (CO) was measured using the thermodilution method and cardiac index (CI) was calculated as CO/body surface area (L/min/m^2). Pulmonary vascular resistance (PVR) was calculated as (mPAP-PCWP)/CO and expressed in Woods Units (WU). The transpulmonary pressure gradient (TPG) was calculated as mPAP-PCWP.

Based on current guidelines PAH was defined as mPAP ≥25mm Hg at rest or ≥30mm Hg during exercise, with PCWP <15mm Hg and PVR >3WU.

CMR imaging

CMR imaging was undertaken in the supine position with a 1.5T scanner (Intera, Philips, Best, the Netherlands) and a five element cardiac synergy coil. Imaging included: 1) imaging of ventricular function with a cine steady state free precession (SSFP) sequence in contiguous short-axis slice covering the entire left ventricle which enabled quantification of right and left ventricular volumes using established quantitative post-processing techniques [19] and comparison to normal values [20]. Typical imaging parameters were TR/TE: 2.9/1.5 ms, flip angle 60°, 30 time frames per cardiac cycle, pixel size 1.4 x 1.4 mm, slice thickness 8 mm and slice gap 0 mm. 2) flow measurement in the ascending aorta or pulmonary trunk using a through-plane phase contrast velocity encoded sequence which enables quantification of effective stroke volume [21]. Typical imaging parameters were TR/TE: 8.7/5.3 ms, slice thickness 6 mm, number of time frames per cardiac cycle 35, pixel size 1.2 x 1.2 mm, velocity encoding gradient (VENC) 200 cm/s, flip angle 15°. 3) oedema imaging with a T2-weighted short tau inversion recovery sequence [22]. Typical imaging parameters were TR/TE: 2 heart beats/100 ms, number of averages 2, inversion time 180 ms, pixel size 1.5 x 1.5 mm; slice 8

mm, slice gap of 2 mm. Parallel imaging with a sensitivity encoding factor 1 was used to minimize signal inhomogeneities due to differences in coil sensitivity. 4) infarct/fibrosis imaging undertaken at least 10 minutes after intravenous contrast injection (0.2 mmol/kg body weight, gadoteric acid, Gothia Medical, Billdal, Sweden) with a T1-weighted inversion recovery sequence set to null the signal in normal myocardium [23]. Typical imaging parameters were: TR/TE: 4/1.3 ms, flip angle 15°, pixel size 1.3 × 1.3 mm slice gap 0 mm and slice thickness 8 mm. Acquisition was set to mid diastole and the inversion time was set to null normal myocardium. Right ventricular hypertrophy and regional wall motion abnormalities were assessed visually by an experienced observer blinded to the clinical characterization. A region of infarct or fibrosis was confirmed in at least two contigous or orthogonal slices. SSc no PAH patients and CTD-PAH patients were compared to established normal reference values [24, 25].

Statistics

The exact binomial test was used to calculate if the number of individuals with a pathological test was significantly greater than expected based on the distribution in the controls. Comparison of groups was done by calculating the 95% confidence intervals for the cases. If the intervals overlap the references' mean it was considered to differ significantly. Associations between variables were analysed using Spearman's correlation. A p-value < 0.05 was considered significant.

RESULTS

The demographic features of the study population are described in Table 1.

CTD-PAH patients

Enlarged right sided dimensions in CTD-PAH patients

Compared to a normal reference population, patients diagnosed with CTD-PAH displayed smaller left ventricular end diastolic volume, smaller left ventricular stroke volume and smaller left ventricular ventricle mass index. They also had a reduced stroke volume into the aorta and pulmonary artery. Furthermore, patients diagnosed with CTD-PAH had larger right ventricular end diastolic volume and larger right ventricular end systolic volume. However they had smaller right ventricular stroke volume index, and small right ventricular ejection fraction. In fact, no patient with CTD-PAH had a normal right ventricular end systolic volume or right ventricular ejection fraction (Table 2; Figure). Right ventricular hypertrophy, global dysfunction, regional dysfunction and valvular dysfunction were also often seen in patients with CTD-PAH (Table 3).

Right sided dimensions reflect the hemodynamic findings of the right heart catheterisation

In addition to the 9 CTD-PAH patients, also 2 of the SSc no PAH patients were examined by RHC because of a suspicion of PAH. In these 2 patients PAH was excluded. The correlation between the right heart measurements by CMR and the hemodynamic findings was calculated in 11 patients (Table 4). Pulmonary vascular resistance, which is the underlying cause of PAH, correlated with right ventricular end systolic volume and right ventricular ejection fraction but not with the right ventricular end diastolic volume.

Fibrosis in the right ventricular insertion point in CTD-PAH patients

In 8 out of 9 patients with CTD-PAH, left ventricular fibrosis was seen midmurally or epicardially, inferoseptally, in the right ventricular insertion point, whereas only one of the SSc no PAH patients displayed this feature (Figure). This patient was diagnosed with CTD-PAH 20 months later upon developing dyspnoea and an increased tricuspid gradient. At the time of CMR he had no dyspnea, spirometry showed vital capacity 95 % of predicted,

diffusion capacity for carbon monoxide was 51 % of predictec, serum NT-ProBNP was 541 pg/mL, and the echocardiography showed signs of diastolic dysfunction and a tricuspid gradient of 24 mmHg. Fibrosis was also seen in other parts of the myocardium in the SSc no PAH patients (Table 3). One SSc patient displayed fibrosis in the left ventricle with a transmural distribution midventricularly and a subendocardial distribution apically and anterolaterally. The localisation was concordant with the coronary angiogram which showed an occlusion of a large intermediate branch. Thus, the fibrosis was the result of a myocardial infarction and not related to SSc. In addition, 3 patients from the group CTD-PAH displayed fibrosis in other parts of the myocardium. In 2 patients the fibrosis was due to myocardial infarction. The third patient was a 46 yrs old patient with juvenile idiopathic arthritis. He had severe CTD-PAH with CI 1.2 L/min/m^2 and PVR 18.8 WU and displayed diffuse fibrosis throughout the right ventricle but none in the left ventricle.

SSc no PAH patients

Frequent but mild CMR changes in SSc no PAH patients

The SSc no PAH patients without a suspicion of PAH displayed CMR pathology in both right and left ventricular dimensions although less pronounced than in patients with CTD-PAH (Table 2-3). The patient with right ventricular hypertrophy but without CTD-PAH suffered from scleroderma renal crisis.

DISCUSSION

In this study, CMR measurements of right ventricular volumes and function show severe pathology in patients with CTD-PAH. However, SSc no PAH patients have similar but milder findings. It is worth noticing that right ventricular end diastolic volume and right ventricular ejection fraction was abnormal in all patients with CTD-PAH as signs of right ventricular

failure. Also abnormal left ventricular volumes and function were present in CTD-PAH patients as well as in SSc no PAH patients. The reason for left sided pathology may be different in these two groups. The CTD-PAH patients have a left ventricle that is compressed by the overfilled right ventricle whereas the SSc no PAH patients may have left ventricular diastolic and systolic dysfunction unrelated to the right ventricle. The left ventricle dysfunction may be caused by systemic hypertension, myocardial ischemia, or speculatively by diffuse fibrosis not visualised by CMR.

A study by Hachulla *et al* did not show differences in right ventricle ejection fraction between patients with or without PAH [12]. In our study both patient groups had impaired right ventricle function although PAH patients were more severely affected. Of interest is that our SSc patient who later developed CTD-PAH had the smallest right ventricular ejection fraction in the group of SSc patients, already 20 months before the diagnosis of CTD-PAH. Bezante *et al* showed differences in right ventricle ejection fraction between controls and SSc patients [10] and this is an important finding as it may be an early sign of increased right ventricular pressure due to PAH..

The unique advantage of CMR was seen when tissue properties were assessed. Fibrosis in the right ventricle insertion point was seen in 8 CTD-PAH patients but in only one of the SSc no PAH patients. In a study of PAH patients by McCann *et al* [26], fibrosis, seen as hyperenhancement, was noticed in all 10 patients submitted for annual follow-up and in all 5 patients with newly diagnosed PAH. Four of these patients had PAH associated with SSc and 11 had idiopathic PAH (group 1.1 in the Venice classification [16]). In a cross-sectional study of 25 patients with idiopathic PAH, CTD-PAH or chronic thromboembolic pulmonary hypertension (CTEPH; group 4 in the Venice classification [16]) 23 patients displayed fibrosis in the right ventricle insertion point, and it extended into the interventricular septum in 16 patients [27]. It is unknown when the fibrosis in the right ventricular insertion point first

may be noticed. The findings in our CTD-PAH group, consisting solely newly diagnosed PAH patients, implies that it may be an early event. This is supported by the finding of fibrosis in the right ventricular insertion point in one SSc patient without symptoms but who was later diagnosed with CTD-PAH. This finding may be worth looking for in a screening situation. A CMR investigation directed at searching for fibrosis in the right ventricular insertion point may thus be used to improve the selection of SSc patients eligible for RHC. This has the advantage of potentially leading to earlier diagnosis and possibly also to an improved survival. Fibrosis in the right ventricular insertion point is likely related to the increased tension caused by the pressure induced dilation of the right ventricle. Both fibrosis of the right ventricular insertion point and enlarged right sided dimensions may be seen secondary to other causes of increases pulmonary vascular resistance. However, in the case of patients with SSc, these conditions are often elucidated by other parts of the investigational algorithm.

In SSc patients, fibrosis in other parts of the myocardium may be seen and these changes may be caused by other mechanisms. In a study of 41 SSc patients, myocardial fibrosis, most often located in the midwall, was seen in 66% of the patients [9]. In that study, disease duration was around 10 years and a majority of the patients were classified as dcSSc as opposed to our cohort of 25 SSc patients with shorter disease duration and only 2 patients classified as dcSSc. It is likely that the occurrence of myocardial fibrosis, although its cause is unknown in SSc, is associated with disease progress during the first years in a similar way as skin fibrosis and pulmonary fibrosis. It is also possible that the low prevalence of dcSSc patients in the present study contributes to the less common finding of myocardial fibrosis. This might explain the striking difference between our cohort of SSc cases and the study by Tzelepis *et al* [9].

Table 4 illustrates that there is a relation between invasive and non invasive assessment of CTD-PAH patients. In this case it is exemplified by the relation between right ventricle end

diastolic volume index, right ventricle end systolic volume index and right ventricle ejection fraction measure by CMR, and TPG, right atrial pressure and PVR measured by right heart catheterization. Further studies are warranted to elucidate whether a non-invasive, less expensive and less time consuming method such as CMR could replace right heart catheterization in the follow-up after diagnosis of CTD-PAH. Notably, CMR imaging with fat suppression was not performed. In infarct/fibrosis images by CMR, fat also displays bright signal intensities. Although unlikely, the bright signal intensities interpreted as fibrosis in the right ventricular insertions could also theoretically be fat, and this is a limitation in the current study.

In summary, CMR shows severe changes in right ventricular volumes and function, but also fibrosis in the right ventricle insertion point at an early time point in patients with CTD-PAH, and further evaluation is warranted to determine whether this finding is of value to screen for early signs of PAH in SSc. Similar abnormalities, although much less severe, may be seen already at diagnosis of SSc. Which SSc patients should be subjected to CMR, and when during the disease course remains to be elucidated. Our study suggests that valuable information may be obtained by CMR also in SSc patients without PAH and even more information may be obtained when examining patients with risk factors for, or a suspicion of CTD-PAH.

ACKNOWLEDGEMENTS

This work was supported in part by grants from the Lund University Faculty of Medicine, the Swedish Rheumatism Association, Gustaf V's 80 years Fund, the Österlund Foundation, the Swedish Heart and Lung Foundation, the Koch Foundation, the Swedish Medical Research Council, and the Region of Scania .

REFERENCES

1. LeRoy EC, Black C, Fleischmajer R, Jablonska S, Krieg T, Medsger TA Jr, et al. Scleroderma (systemic sclerosis): classification, subsets and pathogenesis. J Rheumatol 1988; 15:202-5.
2. Bryan C, Howard Y, Brennan P, Black C, Silman A. Survival following the onset of scleroderma: results from a retrospective inception cohort study of the UK patient population. Br J Rheumatol 1996; 35:1122-6.
3. Hesselstrand R, Scheja A, Akesson A. Mortality and causes of death in a Swedish series of systemic sclerosis patients. Ann Rheum Dis 1998; 57:682-6.
4. Lee P, Langevitz P, Alderdice CA, Aubrey M, Baer PA, Baron M, et al. Mortality in systemic sclerosis (scleroderma). Q J Med 1992; 82:139-48.
5. Simeón CP, Armadans L, Fonollosa V, Solans R, Selva A, Villar M, et al. Mortality and prognostic factors in Spanish patients with systemic sclerosis. Rheumatology (Oxford) 2003; 42:71-5.
6. Steen VD, Medsger TA. Changes in causes of death in systemic sclerosis, 1972-2002. Ann Rheum Dis 2007; 66:940-4.
7. Ferri C, Emdin M, Nielson H, Bruhlmann P. Assessment of heart involvment. Clin Exp Rheumatol 2003; 21 (3 Suppl 29):S24-8.
8. Plastiras SC, Kelekis N, Tzelepis GE. Magnetic resonance imaging for the detection of myocardial fibrosis in scleroderma. N Engl J Med 2006; 354:2194-6.
9. Tzelepis GE, Kelekis NL, Plastiras SC, Mitseas P, Economopoulos N, Kampolis C, et al. Pattern and distribution of myocardial fibrosis in systemic sclerosis. A delayed enhanced magnetic resonance imaging study. Arthritis Rheum 2007;56: 3827-36.

10. Bezante GP, Rollando D, Sessarego M, Panico N, Setti M, Filaci G, et al. Cardiac magnetic resonance imaging detects subclinical right ventricular impairment in systemic sclerosis. J Rheumatol 2007; 34:2431-7.
11. Nassenstein K, Breuckmann F, Huger M, Ladd SC, Schlosser T, Kreuter A, et al. Detection of myocardial fibrosis in systemic sclerosis by contrast-enhanced magnetic resonance imaging. Rofo 2008; 180:1054-60.
12. Hachulla AL, Launay D, Gaxotte V, de Groote P, Lamblin N, Devos P, et al. Cardiac magnetic resonance imaging in systemic sclerosis: a cross-sectional observational study of 52 patients. Ann Rheum Dis 2009; 68:1878-84.
13. Kobayashi H, Yokoe I, Hirano M, Nakamura T, Nakajima Y, Fontaine KR, et al. Cardiac magnetic resonance imaging with pharmacological stress perfusion and delayed enhancement in asymptomatic patients with systemic sclerosis. J Rheumatol 2009; 36:106-12.
14. Allanore Y, Meune C, Vignaux O, Weber S, Legmann P, Kahan A. Bosentan increases myocardial perfusion and function in systemic sclerosis: A magnetic resonance imaging and tissue-doppler echography study. J Rheumatol 2006; 33:2464-9.
15. Hsu VM, Moreyra AE, Wilson AC, Shinnar M, Shindler DM, Wilson JE, et al. Assessment of pulmonary arterial hypertension in patients with systemic sclerosis: comparison of noninvasive tests with results of right-heart catheterization. J Rheumatol 2008; 35:458-65.
16. Simonneau G, Galiè N, Rubin LJ, Langleben D, Seeger W, DomenighettiG, et al. Clinical classification of pulmonary hypertension. J Am Coll Cardiol 2004 ; 43(12 Suppl S):5S-12S.

17. Masi AT, Medsger TA Jr., Altman RD, D'Angelo WA, Fries JF, LeRoy EC, et al. Preliminary criteria for the classification of systemic sclerosis (scleroderma). Subcommittee for scleroderma criteria of the American Rheumatism Association Diagnostic and Therapeutic Criteria Committee. Arthritis Rheum 1980; 23:581-90.
18. LeRoy EC, Medsger TA Jr. Criteria for the classification of early systemic sclerosis. J Rheumatol 2001; 28:1573-6.
19. Pennell DJ. Ventricular volume and mass by CMR. J Cardiovasc Magn Reson 2002; 4:507-13.
20. Maceira AM, Prasad SK, Khan M, Pennell DJ. Normalized left ventricular systolic and diastolic function by steady state free precession cardiovascular magnetic resonance. J Cardiovasc Magn Reson 2006; 8:417-26.
21. Arheden H, Saeed M, Higgins CB, Gao DW, Bremerich J, Wyttenbach R, et al. Measurement of the distribution volume of gadopentetate dimeglumine at echo-planar MR imaging to quantify myocardial infarction: comparison with 99mTc-DTPA autoradiography in rats. Radiology 1999; 211:698-708.
22. Abdel-Aty H, Zagrosek A, Schulz-Menger J, Taylor AJ, Messroghli D, Kumar A, et al. Delayed enhancement and T2-weighted cardiovascular magnetic resonance imaging differentiate acute from chronic myocardial infarction. Circulation 2004; 109:2422-6.
23. Simonetti OP, Kim RJ, Fieno DS, Hillenbrand HB, Wu E, Bundy JM, et al. An improved MR imaging technique for the visualization of myocardial infarction. Radiology 2001; 218:215-23.
24. Maceira AM, Prasad SK, Khan M, Pennell DJ. Reference right ventricular systolic and diastolic function normalized to age, gender and body surface area from steady-state free precession cardiovascular magnetic resonance. Eur Heart J 2006; 23:2879-88.

25. Maceira AM, Prasad SK, Khan M, Pennell DJ. Normalized left ventricular systolic and diastolic function by steady state free precession cardiovascular magnetic resonance. J Cardiovasc Magn Reson 2006; 3:417-26.
26. McCann GP, Gan CT, Beek AM, Niessen HW, Vonk Noordegraaf A, van Rossum AC. Extent of MRI delayed enhancement of myocardial mass is related to right ventricular dysfunction in pulmonary artery hypertension. AJR Am J Roentgenol 2007; 188:349-55.
27. Blyth KG, Groenning BA, Martin TN, Foster JE, Mark PB, Dargie HJ, et al. Contrast enhanced-cardiovascular magnetic resonance imaging in patients with pulmonary hypertension. Eur Heart J 2005; 26:1993-9.

LEGENDS TO FIGURE

FIGURE

Examples of cardiovascular magnetic resonance (CMR) images from a patient with pulmonary arterial hypertension (PAH) and abnormal CMR findings, and a patient with systemic sclerosis (SSc) and normal CMR findings. Top two rows shows long axis and short axis CMR images in end diastole and end systole in a patient with PAH and right ventricular (RV) enlargement. Delayed contrast enhanced CMR shows fibrosis at the RV insertion point of the left ventricle (LV) (white spot indicated by arrow). Bottom two rows show corresponding images in a patient with SSc and normal CMR findings.

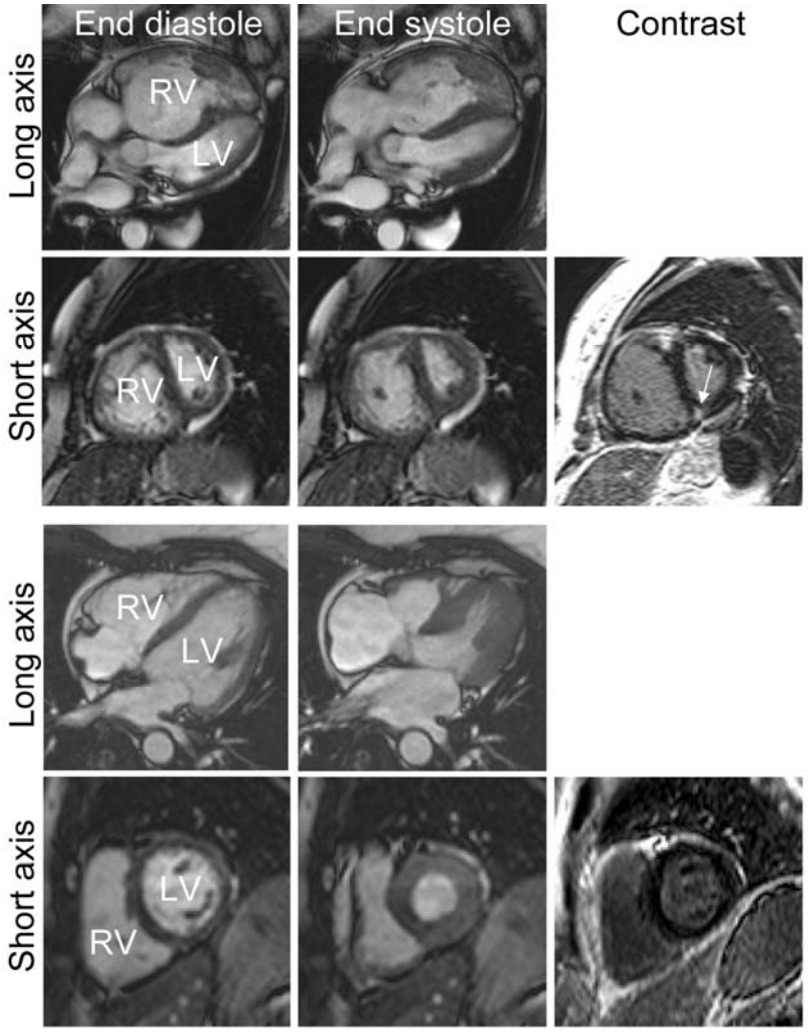
End diastole
End systole
Contrast
Long axis
RV
LV
Short axis
RV
LV
Long axis
RV
LV
Short axis
LV
RV

TABLES

TABLE 1

Description of the study populations

	SSc no PAH patients	CTD-PAH patients
male/female (n)	6/19	7/2
Centromeric abs: positive/negative (n)	15/10	4/5
WHO class I/II/III/IV (n)	13/10/1/1	0/1/5/3
Age at diagnosis (yrs)	56.4 (47.8-64.8)	68.3 (59.6-76.0)
Disease duration* (yrs)	2.5 (0.9-10.6)	4.8 (2.6-8.7)
Modified Rodnan skin score (points)	3.0 (0.75-5.5)	1.0 (0-2.25)
sPAP (mm Hg)	25.4 (21.0-30.6)	74.6 (73.6-82.2)
mPAP (mmHg)	n/a	40.0 (35.0-45.0)
PVR	n/a	6.6 (5.2-9.4)
VC (p%)	93.0 (81.0-99.5)	74.5 (60.5-91.0)
DL_{CO} (p%)	79.5 (59.5-89.75)	24.5 (22.5-31.5)
6 minutes walking distance (m)	n/a	240 (144-264)
NT-ProBNP (pg/mL)	213 (69.5-1153)	3006 (1662-6766)

Abbreviations: SSc: systemic sclerosis; CTD-PAH: pulmonary arterial hypertension associated with connective tissue disease; dcSSc: diffuse cutaneous SSc, lcSSc: limited cutaneous SSc; susp SSc: suspected SSc; abs: antibodies; sPAP: estimated systolic pulmonary artery pressure by echocardiography; mPAP: mean pulmonary arterial pressure by right heart catheterisation; PVR: pulmonary vascular resistance; VC: vital

capacity; p%: % of predicted; DL_{CO}: diffusion capacity for carbon monoxide; NT-ProBNP: N-terminal Pro brain natriuretic peptide; n/a: not applicable. * Disease duration from first non Raynaud's manifestation.

Continuous variables are presented as median (interquartile range).

TABLE 2

Comparison between reference values, SSc patients and PAH patients.

Variable	Reference [24, 25]	SSc no PAH patients		CTD-PAH patients	
	mean (SD)	mean (95% CI)	pathological/normal	mean (95% CI)	pathological/normal
LVEDVI (ml/m^2)	78 (8.8)	76.2 (70.3-82.1)	5/20***	59.8 (52.4-67.2)***	6/3**
LVESVI (ml/m^2)	26 (5.1)	28.6 (25.3-31.9)	4/21***	24.0 (19.1-28.9)	1/8
LVSVI (ml/m^2)	52 (6.2)	47.8 (44.1-51.5)*	5/20***	33.8 (26.9-40.7)***	5/4***
LVEF (%)	67 (4.6)	62.8 (60.2-65.3)**	4/21***	59.4 (51.0-67.8)	3/6**
LV massI (g/m^2)	69 (8.1)	69.8 (61.6-78.0)	5/20***	58.2 (50.2-66.0)**	4/5***
SV effective aorta (ml)	95 (14)	75.4 (69.1-81.7)***	6/19***	61.0 (45.1-76.9)***	5/4***
RVEDVI (ml/m^2)	78 (11)	72.7 (67.9-77.5)*	1/23	108 (86.3-129)**	4/5***
RVESVI (ml/m^2)	27 (7)	29.0 (25.2-32.8)	3/21*	72.5 (53.5-91.5)***	9/0***
RVSVI (ml/m^2)	51 (7)	43.7 (41.1-46.3)***	3/21*	35.8 (29.5-42.1)***	5/3***
RVEF (%)	66 (6)	60.8 (57.5-64.1)**	5/19***	34.3 (28.0-40.6)***	9/0***
SV effective PA (ml)	94 (15)	76.0 (70.0-82.0)***	3/18*	51.2 (34.6-67.8)***	5/1***

Abbreviations: LV: left ventricle; RV: right ventricle; EDV: end diastolic volume; ESV: end systolic volume; SV: stroke volume; SV effective: SV measured by CMR velocity-enchoded flow quantification in a great vessel; I: indexed to body surface area; EF: ejection fraction; PA: pulmonary artery; ns: not significant.

*p<0.05; **p<0.01; ***p<0.001; p-values for means refer to comparison between the patients as a group and the reference population.

Pathological refers to the number of patients falling outside the 95% CI of the reference population.

TABLE 3

CMR findings in patients with or without PAH

	SSc no PAH patients	CTD-PAH patients
	n/25 (%)	n/9 (%)
myocardial infarction	1 (4)	2 (22)
fibrosis	2 (8)	8 (89)
oedema	1 (4)	4 (44)
hypertrophic RV	1 (4)	8 (89)
hypertrophic LV	2 (8)	0 (0)
global dysfunction	2 (8)	8 (89)
regional dysfunction	1 (4)	5 (56)
valvular dysfunction	0 (0)	3 (33)
pericardial effusion	2 (8)	1 (11)

Abbreviations: RV: right ventricle; LV: left ventricle

TABLE 4

Correlations between hemodynamic findings on the right heart catheterisation and CMR measurements in 9 patients with CTD-PAH and 2 patients with SSc, without PAH.

	RVEDVI (ml/m^2)	RVESVI (ml/m^2)	RVEF (%)
	r_s	r_s	r_s
mPAP (mmHg)	0.57	0.62*	-0.63*
TPG (mmHg)	0.64*	0.69*	-0.83**
RAP (mmHg)	0.77**	0.72*	-0.59
CO (L/min)	-0.04	-0.13	0.12
CI (L/min/m^2)	-0.14	-0.24	0.16
PVR (WU)	0.52	0.67*	-0.72*

RV: right ventricle; EDV: end diastolic volume; I: indexed to body surface area; ESV: end systolic volume; EF: ejection fraction; mPAP: mean pulmonary arterial pressure: TPG: transpulmonary pressure gradient; RAP: right atrial pressure; CO: cardiac output; CI: cardiac index; PVR: pulmonary vascular resistance; *$p<0.05$; **$p<0.01$; r_s: Spearmans rho; WU: Woods Units.